

Interference Management and Six-Sector Macrocells for Performance Improvement in Femto–Macro Cellular Networks

Hashem Kalbkhani · Sahar Jafarpour-Alamdari ·
Vahid Solouk · Mahrokh G. Shayesteh

Published online: 17 October 2013
© Springer Science+Business Media New York 2013

Abstract Femtocells are considered as a solution for indoor high data rate demands. Interference mitigation is a fundamental challenge in two-tier femto–macrocell networks. In this paper, we consider six-sector macrocell layout for reducing the co-tier interference in the macrocell network and cross-tier interferences from macrocell to femtocell network. As interference reduces, the whole of available spectrum can be used in each macrocell which increases the spectrum efficiency. We also consider interference-level algorithm to allocate resource for femtocell in which macrocell uses the whole of spectrum. In the coverage area of each sector, femtocell uses a portion of the spectrum that is not used by the macrocell users. This approach ignores the high co-channel interference from the macrocell network to the femtocell network and vice versa in each sector. Simulation results show that the proposed layout and interference management scheme reduce the downlink interference and increase the efficiency of the orthogonal frequency division multiple access (OFDMA)-based femtocell and macrocell. Consequently, system throughput and outage probability are improved significantly.

Keywords Femtocell · Interference · Outage probability · Resource block allocation · Sector · Throughput

1 Introduction

With the increasing capacity and demand for high data rate services in wireless networks and considering the fact that most of data and voice services take place in the indoor environments, the incapability of the conventional cellular systems in providing services for indoor

H. Kalbkhani (✉) · S. Jafarpour-Alamdari · M. G. Shayesteh
Department of Electrical Engineering, Urmia University, 10th Km Nazloo Road, Urmia,
West Azerbaijan State, Iran
e-mail: st_h.kalbkhani@urmia.ac.ir

V. Solouk
Department of IT and Computer Engineering, Urmia University of Technology, Urmia, Iran

users is foreseen due to the poor propagation coverage [1]. The use of two-tier networks structure comprising a conventional cellular network overlaid with short range hotspots can be used especially in indoor. Femtocells have been introduced as a solution to the mentioned shortcomings [2].

Femtocells are small in size, short range, low cost, and low power home base stations deployed over macrocell networks to provide improved coverage for indoor users and enhance the capacity of the whole system [1]. Femtocells are installed by the costumers and connected to the network over a broadband communications links such as digital subscriber line (DSL) or fiber optic links [1]. The technology has brought concerns both from user side and from the operator side. While users are placed as the main objectives of deploying femtocells, as enjoying better signal quality, throughput, and affordable power saving, operators also benefit from greater network capacity as well as the spectral efficiency [3]. Despite of all benefits mentioned, the technology introduces some limitations; among them cross-tier interference mitigation is known as a serious challenge in the femto–macrocell co-deployment environments with both of orthogonal and shared channel allocations [3]. The significance of this issue has been enticed considerable attentions over the recent era, adequate to bring great deal of the recent studies to propose a range of interference mitigation techniques.

The contributions of this study are as follows:

- (a) *Introducing New Cell Layout for Femto–Macrocell Networks* At first new cell layout for two-tier femto-cellular networks is presented and its specifications are explained in more detail.
- (b) *Co-tier Interference Analysis* Analyzing the received interference from macrocell to femtocell network is the next contribution of this work.
- (c) *Resource Block Allocation to Femtocell Based on the Interference Level* Based on the calculated cross-tier interferences, three different algorithms for resource block allocation to femtocell are considered.
- (d) *Obtaining Cellular Network Performance in terms of Throughput and Outage Probability* After resource block allocation to femtocell by different algorithms, the efficiency of each algorithm is investigated and compared with other cell layouts of macrocell network.

The rest of the paper is organized as follows. Related works are presented in Sect. 2. System and channel models are described in Sect. 3. Throughput and outage probability are derived in Sect. 4. The proposed resource allocation scheme and performance metrics are explained in Sect. 5. Simulation results are provided in Sect. 6. Finally, Sect. 7 concludes the paper.

2 Related Works

In [4] a dynamic frequency-reuse method along with self-organizing network were introduced in order to reduce interference. Power control is another approach to control the interference. For example in [2] femtocell users reduce their transmit powers in order to reduce their uplink interference to the macrocell base station. Moreover, several studies have proved that sectorized cell schemes are more practical and efficient to reduce interference [5,6], so that they can be considered for femto–macrocell networks. In [6], only downlink outage probability has been investigated in three-sector macrocell layout. The results show that using three-sector macrocell layout reduces the cross-tier interferences. Therefore, utilizing three-sector macrocells instead of macrocells with omnidirectional antennas improves the outage probability of femtocell networks. The algorithm presented in [7] used different time slots to allocate

frequency band to femtocell and macrocell networks and by this approach manages interference in femto–macrocell network. Since time hopping algorithms require perfect synchronization between femtocell and macrocell, increasing the number of femtocells degrades the performance of this algorithm. Also, femtocells are turned on/off by users which can affect time hopping approaches. Interference management techniques for both downlink and uplink of UMTS-based femtocells were presented in [8]. Femtocell carrier selection and femtocell transmission power for downlink and interference management, adaptive attenuation at the femtocell, and limiting the transmission power of femtocell users for uplink were proposed. Cognitive interference management approach to reduce co-channel interference among femtocells was introduced in [9] that allows each femtocell to access all available bands but requires good femtocells with high throughput to donate some bands to poor ones. Fractional frequency reuse (FFR) was used in [10] to mitigate co-tier in dense femtocell environments. Frequency reuse factor (FRF) was adjusted with the aid of femtocell location information. Optimal power allocation for femtocells with different orthogonal sub-bands based on the analysis of macrocell interferences was presented in [11]. In [12] a framework for radio coverage prediction and system level simulation for WiMAX femto–macrocell scenarios was proposed. Furthermore, a method for interference avoidance based on dynamic frequency planning was presented. Distributed and self-organizing femtocell management architectures, that consist of three control loops were also proposed in [13].

3 System and Channel Models

In this work, downlink of orthogonal OFDMA-based hierarchical femto–macrocell overlay cellular network is considered. As shown in Fig. 1, the central hexagonal macrocell (M_0) is surrounded by two-tier of hexagonal macrocells, where $M_{t,j}$ indicates the j th macrocell in the t th tier. Since the distance between the macrocells of the third and higher tiers from central macrocell is large, the effects of those macrocells are not taken in account. Hence, according to Fig. 1, the cellular system has a total of 19 macrocells where M_0 is located at the 0th tier, six of macrocells belong to the first tier, and the other 12 belong to the second tier. In this paper, we consider the coverage area of M_0 . Each macrocell consists of six sectors. Noting Fig. 1, $Se_{t,j,k}$ indicates the k th sector of the j th macrocell of the t th tier. The macro base station (MBS) of M_0 is located at the origin $(0, 0)$ of R^2 plane. The radius of each macrocell is equal to R_m and the inter-MBS distance is $2R_{Id}$ where $R_{Id} = \sqrt{3}R_m/2$. Hence, the locations of MBSs of $M_{t,j}$ are $[2R_{Id} \cos(\frac{\pi}{3}(j-1)), 2R_{Id} \sin(\frac{\pi}{3}(j-1))]$ and $[4R_{Id} \cos(\frac{\pi}{6}(j-1)), 4R_{Id} \sin(\frac{\pi}{6}(j-1))]$ in the first and second tiers, respectively.

We assume that macro user equipment (MUE) is uniformly distributed across each macrocell. Using directional antennas reduces interference; therefore, the entire available spectrum can be used in each macrocell. Consequently, considering Fig. 2, the available spectrum is divided into six equal parts and each part is assigned to one sector. Hence, frequency reuse factor (FRF) is one. In OFDMA-based systems, the basic resource unit that can be allocated to each user is resource block (RB) [14]. It is assumed that all subcarriers in each RB are transmitted with the same power.

Macrocell is assumed to be fully loaded by all available RBs at any time in each sector. In OFDMA-based cellular systems, by assigning at most one user per RB in each cell, the intra-cell interference is avoided in macrocell network [2].

Indoor femtocells are considered in closed-access service mode that serve indoor femto user equipment (FUE) [3]. In this case, only the authorized FUE can connect to femto access point (FAP) and the other FUEs and MUEs do not have permission to connect to FAP. FAPs

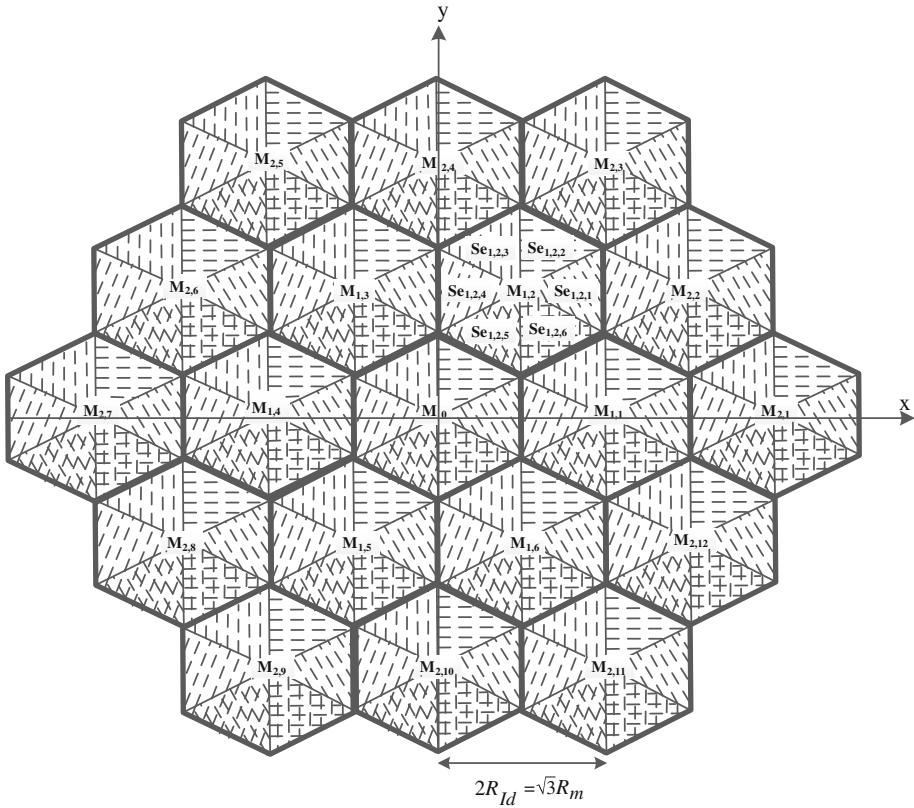


Fig. 1 Macrocell network layout

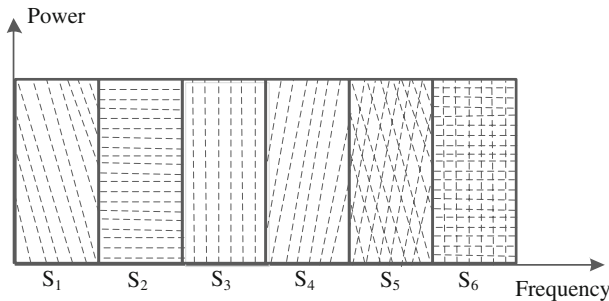


Fig. 2 Sub-band allocation to macrocell in this study

are randomly placed in the macrocell coverage area. Femtocell coverage area is considered as a disk with radius R_F where FAP is placed at the center of disk. The bandwidth and time duration of each RB are restricted [14]. Thus, it can be assumed that all subcarriers of each RB experience the same log-normal (LN) shadowing and frequency-flat Rayleigh fading [2]. Shadowing and fading coefficients across each RB are constant [15], but may vary from one RB to another. IMT-2000 channel model [16] for radio propagation is used. Path losses (PLs) for different links in IMT-2000 are presented in Table 1, where f_c indicates the carrier

Table 1 PLs for different links in the IMT-2000 propagation model

Link (transmitter/receiver)	Wall loss	Fixed loss	Path loss exponent	Path loss
MBS/MUE	N/A	$\phi_M = 10^{-7.1} f_c^3$	α_M	$\phi_M d^{\alpha_M}$
MBS/FUE	ξ	$\phi_{MF} = \phi_M \xi$	α_{MF}	$\phi_{MF} d^{\alpha_{MF}}$
Serving FAP/FUE	N/A	$\phi_F = 10^{3.7}$	α_F	$\phi_F d^{\alpha_F}$

frequency in MHz, ξ is wall penetration loss, and d is the distance between the transmitter and receiver.

4 Downlink Throughput and Outage Probability

To demonstrate the efficiency of six-sector layout, we evaluate the performance in terms of throughput for both macrocell and femtocell networks and the outage probability for femtocell network.

The throughput of the k th RB is calculated as [17]

$$C_K = \Delta f \times \log_2(1 + \alpha SINR) \tag{1}$$

where Δf is the sub-band spacing (bandwidth of RB) and $\alpha = \frac{-1.5}{\ln(5BER)}$ [17] is a constant for target bit error rate (BER) which is set to 10^{-6} in this study. SINR is signal to interference plus noise ratio of the k th RB. Since the level of noise is smaller than the received interference, the effect of noise is ignored and we consider signal to interference ratio (SIR) of each RB. Finally, the total throughput (C) is calculated as

$$C = \sum_{k=1}^{N_{RB}} C_k \tag{2}$$

where C_k is the throughput of the k th RB, and N_{RB} is the number of RBs.

The outage probability (OP) of an RB is defined as the probability that its SIR be smaller than a pre-defined threshold value γ , that is,

$$OP = \Pr(SIR < \gamma) \tag{3}$$

In the case of multiple RBs, if the SIR of at least one RB becomes smaller than a pre-defined threshold, the user cannot obtain its requested bandwidth which causes outage of femtocell user.

In order to obtain downlink throughput and outage probability, at first SIR should be computed. In the following, we calculate the SIR of RB used by FUE and MUE.

4.1 SIR of Macrocell User Equipment (MUE)

The SIR of MUE is derived by considering the interference from neighboring macrocells. Since the transmitted power from FAP is low, the received interference in MUE from the femtocell network is ignored. The downlink SIR of the MUE that uses RB in the k th sub-band considering polar coordinates is given by

$$SIR_M(k, r, \theta) = \frac{P_M H_M Q_M G_M \phi_M^{-1} r^{-\alpha_M}}{\sum_{t=1}^2 \sum_{j=1}^m A_{t,j} P_M H_{M,t,j} Q_{M,t,j} G_{M,t,j} \phi_M^{-1} d_{t,j}^{-\alpha_M}} \tag{4}$$

$$d_{t,j} = \begin{cases} \sqrt{r^2 + 4R_{Id}^2 - 4rR_{Id} \cos(\theta - \frac{\pi}{3}(j-1))} & t = 1, j = 1 : 6 \\ \sqrt{r^2 + 16R_{Id}^2 - 8rR_{Id} \cos(\theta - \frac{\pi}{6}(j-1))} & t = 2, j = 1 : 12 \end{cases} \tag{5}$$

where $m = 6$ for $t = 1$ and $m = 12$ for $t = 2$. P_M denotes the transmission power of each MBS (it is assumed that all MBSs transmit the same power in all sub-bands). r is the distance between the MUE and the serving MBS, $d_{t,j}$ is the distance between MUE and the j th MBS of the t th tier, ϕ_M is the distance-independent propagation loss, α_M is the path loss exponent from the MBS to the MUE, H_M denotes the exponentially distributed unit-mean channel gain from MBS to MUE [2], $Q_M \sim LN(\zeta \mu_{M,dB}, \zeta^2 \sigma_{M,dB}^2)$ is the log-normal shadowing from the MBS to MUE with $\zeta = 0.1 \times \ln 10$ for scaling [2], and $\mu_{M,dB}$ and $\sigma_{M,dB}$ are the mean and standard deviation values, respectively. G_M is the horizontal antenna gain pattern of each MBS sector in dB which is given by [18]

$$G_M = \max \left\{ -12 \frac{(\theta - \omega_{t,j})^2}{\Theta_{3dB}}, A_s \right\} \tag{6}$$

where $\omega_{t,j}$ denotes the direction of main lobe of the j th sector in the t th tier, Θ_{3dB} is the 3 dB bandwidth of the antenna response, and A_s is the side-lobe level of the response [18]. Also, $A_{t,j}$ is a binary number which is set to one if MUE receives interference from the j th macrocell of the t th tier.

4.2 Femtocell User Equipment (FUE) Downlink Throughput

The SIR of RB from the k th sub-band used by FUE in polar coordinates is obtained as

$$SIR_F(k, r, \theta) = \frac{P_F H_F Q_F \phi_F^{-1} d_F^{-\alpha_F}}{\sum_{t=1}^2 \sum_{j=1}^m \beta_{t,j} P_M H_{MF,t,j} Q_{MF,t,j} G_{M,t,j} \phi_{MF}^{-1} d_{t,j}^{-\alpha_{MF}}} \tag{7}$$

where P_F is the FAP transmission power, d_F is the distance between the FUE and the serving FAP, and ϕ_F and ϕ_{MF} are distance-independent propagation losses from the serving FAP and interfering MBS to FUE, respectively. α_F and α_{MF} are path loss exponents from the serving FAP and interfering MBSs to the FUE, respectively. H_F and H_{MF} denote the exponentially distributed unit-mean channel gains from the serving FAP and interfering MBSs to the FUE, respectively [2]. Log-normal shadowing from the serving FAP and interfering MBSs to FUE are described by $Q_F \sim LN(\zeta \mu_F, \zeta^2 \sigma_F^2)$ and $Q_{MF} \sim LN(\zeta \mu_{MF}, \zeta^2 \sigma_{MF}^2)$, respectively, with $\zeta = 0.1 \times \ln 10$ for scaling [2], and $\mu_{F,dB}$, $\mu_{MF,dB}$ are the mean values and $\sigma_{F,dB}$, $\sigma_{MF,dB}$ are the standard deviations. Also, $\beta_{t,j}$ is a binary number which is set to one if FUE receives interference from the j th macrocell of the t th tier.

5 Proposed Resource Block Allocation to Femtocell

5.1 Design Goals

The aim of this section at first is to analyze the co-tier interference from macrocell to femtocell network in different frequency sub-bands based on the information about the FAP location. Then, according to the interference level, three different algorithms for RB allocation to FUE are considered.

Noting (1) and (3), if the SIR of RB increases, the performance of the two-tier network increases. To maximize the performance of femtocell that is located in the coverage of a macrocell sector, we present resource allocation algorithm which minimizes the cross-tier interference from macrocell to femtocell. For this purpose, the received interferences in FUE considering all possible cases (i.e., all sub-bands) are calculated in order to assign different sub-bands to the FUE. Then, with regard to the order of the interferences, RBs from the sub-band with minimum interference are allocated to the FUE. If more RBs are required, RBs from the second low interference sub-band are assigned to FUE and this procedure continues until the RBs from sub-band with maximum interference are allocated.

Without loss generality, we assume that the femtocell is installed in coverage area of the first sector of the central macrocell (M_0) and can use all sub-bands, except the one that belongs to the macrocell in the first sector. If FUE uses the RBs from the sub-band that belongs to the MUE in the first sector, high cross-tier interference from macrocell in co-channel sub-band causes considerable decrease in the throughput and increase in the outage probability of FUE.

5.2 Random RB Allocation (RRBA)

FUE can randomly choose its RBs from the remaining sub-bands. In the random RB allocation (RRBA), RNC does not send the order of interference of different sub-bands to FAP. Therefore, FAP allocates RBs to FUE from the set of sub-bands {2, 3, 4, 5, 6} without any priority.

5.3 Optimal RB Allocation (ORBA)

Random selection does not guarantee minimum interference in the FUE. In the optimal RB allocation (ORBA), RNC has knowledge about the exact location of FAP in the first sector. Thus for each sub-band, we calculate the interference from macrocell network. It was shown that downlink femto to femto interference is much smaller than downlink macro to femto interference [19]. This is because of much higher transmitting power of MBS than FAP and the double-wall partition loss between indoor femtocells. Hence, in this paper, co-tier femto to femto interference is ignored. Polar coordinates ($0 < r \leq R_m$, $-\pi/6 \leq \theta \leq \pi/6$) are considered for the FUE location. To determine the minimum interference, we obtain cross-tier interference in the k th sub-band from macrocell to FUE by using denominator of (7).

It is worth mentioning that for determining the order of interference of different sub-bands, shadowing and fast fading effects of channel are not considered. Figure 3 presents the received interference in different sub-bands versus the distance of FUE from the origin (r). The curves are obtained using the parameters described in Table 2 (mentioned in the next section). It should be noted that in the specific distance from the origin, the results are averaged on the positive and negative angles (θ), i.e.,

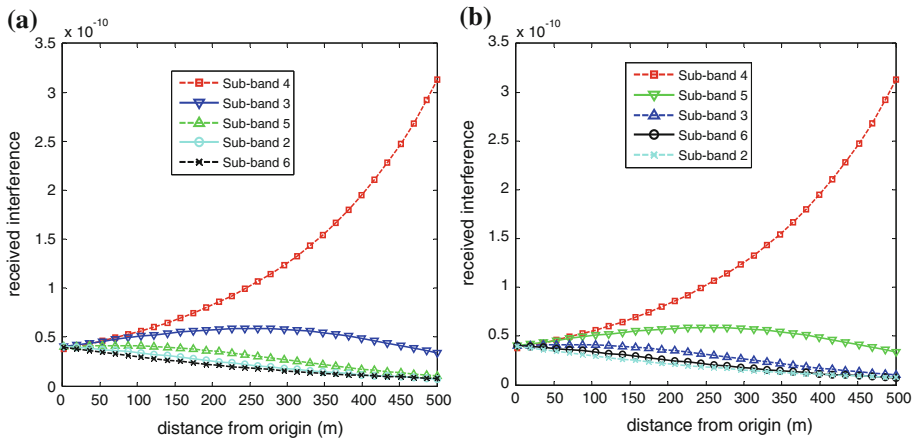


Fig. 3 Received interference in different sub-bands versus the distance of FUE from the origin. **a** Average interference in *negative* angles. **b** Average interference in *positive* angles

$$I_{MF, Pavg}(k, r) = \frac{1}{(\pi/6)} \int_0^{\pi/6} I_{MF}(k, r, \theta) d\theta \tag{8}$$

$$I_{MF, Navg}(k, r) = \frac{1}{(\pi/6)} \int_{-\pi/6}^0 I_{MF}(k, r, \theta) d\theta \tag{9}$$

where $I_{MF, Pavg}(k, r)$ and $I_{MF, Navg}(k, r)$ denote the average interference in the positive and negative angles, respectively. As seen from Fig. 3, sub-band four has the highest interference for both negative and positive angles. Sub-bands six and two have the lowest interference for negative and positive angles, respectively. It is also observed that for small distances ($r < 100$), the received interferences in all sub-bands have about the same values. Therefore, there are no considerable differences between the throughputs and outage probabilities of different sub-bands. As distance increases, the difference between interferences also increases more and throughputs and outage probabilities of different sub-bands become more different. So, interference management in large distances has great effect on the FUE. Hence, by assigning RBs from low interference sub-bands to FUE, the efficiency of femtocell increases which improves the overall efficiency of hierarchical cellular network. In this case, for positive angles, sub-band two has the highest priority. When all RBs of sub-band two are used, FAP allocates the RBs of sub-band six. If FUE needs more RBs, the RBs of sub-bands three, five, and four are used.

5.4 Semi-optimal RB Allocation (SORBA)

In the semi-optimal RB allocation (SORBA), RNC only knows the sector in which FAP is located and does not have information about the exact location of FAP. In Fig. 4, the received interferences from different sub-bands are shown where in different distances, the results are averaged over different angles over the range $-\pi/6 \leq \theta \leq \pi/6$ as

$$I_{MF, avg}(k, r) = \frac{1}{(\pi/3)} \int_{-\pi/6}^{\pi/6} I_{MF}(k, r, \theta) d\theta \tag{10}$$

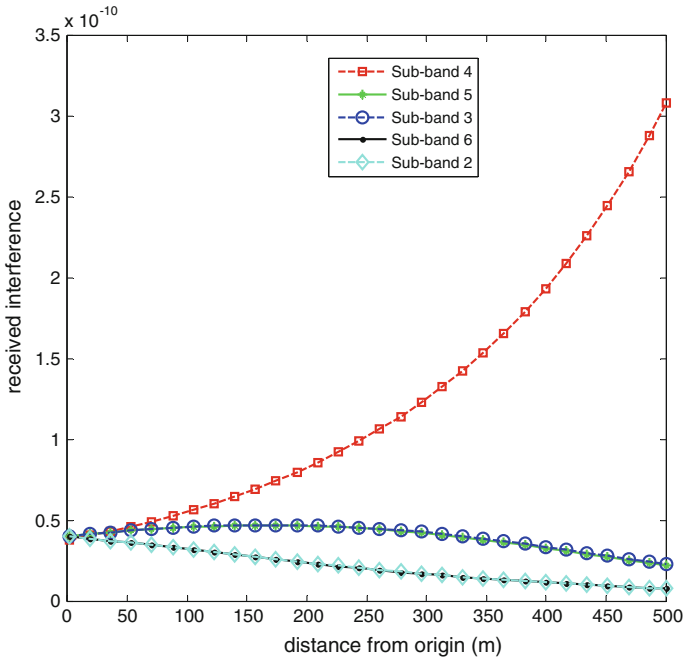


Fig. 4 Received interference in different sub-bands versus the distance of FUE from the origin averaged over the range $-\pi/6 \leq \theta \leq \pi/6$

where $I_{MF,avg}(k, r)$ denotes the average interference in the first sector. It is observed that in the range $-\pi/6 \leq \theta \leq \pi/6$, the received interferences from the sub-bands six and two are the same. Therefore, those RBs that belong to the sub-bands six and two have the same priority. Also, the received interferences in the sub-bands five and three have the same values. In this case, the set of sub-bands two and six have the same priority and FAP starts allocating from the set of these sub-bands. When all RBs of these sub-bands are used, the RBs from the set of sub-bands three and five with the same priority are allocated; note that sub-band four has the lowest priority.

From Figs. 3 and 4, it is evident that if we have more details about FAP and FUE locations in the R^2 plane, more information about macrocell to femtocell co-tier interference are obtained. Therefore, by allocation RBs from low-interference sub-bands, higher SIR at FUE is achieved. FAP connects to radio network controller (RNC) via xDSL line or fiber [1]. Thus, RNC knows the location of each FAP in the R^2 plane.

6 Simulation Results

This section includes the results of Monte Carlo simulations to assess the performance of the proposed heterogeneous cellular networks in terms of throughput and outage probability. The parameters of the proposed system and channel model are presented in Table 2.

Table 2 Parameters of the cellular system used in this study

Parameter	Value	Parameter	Value
Macrocell/femtocell radius (R_m/R_f)	500/20 m	Carrier frequency (f_c)	2,000 MHz
MBS transmitter power (P_M)	43 dBm	Wall loss (ξ)	10 dB
FAP transmitter power (P_F)	20 dBm	α_F	3
Total available bandwidth	20 MHz	α_M, α_{MF}	4
Bandwidth of RB (Δf)	200 kHz	$\sigma_F, \sigma_M, \sigma_{MF}$	4, 8, 10 dB
Θ_{3dB} for three-sector/six-sector	$35^\circ/70^\circ$	A_S for three-sector/ six-sector	-20 dB/-23 dB

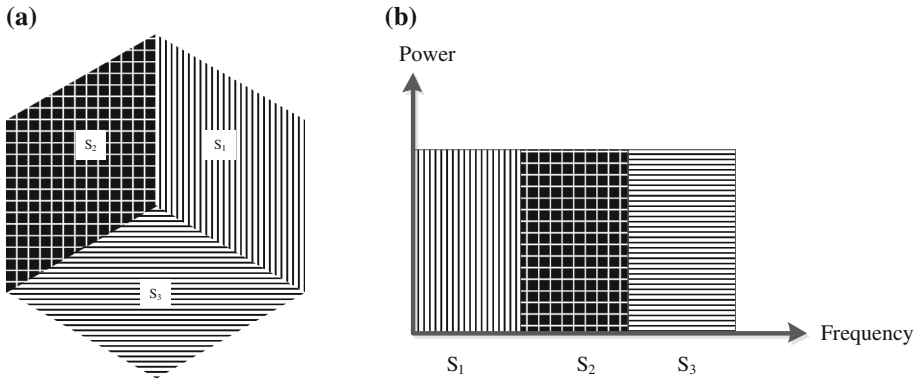


Fig. 5 Three-sector macrocell layout with frequency partitioning into different sub-bands. **a** Three-sector macrocell. **b** Sub-band allocation to different sectors

The available frequency band is divided into 100 RBs each with 200 kHz bandwidth. We assume that the macrocell is fully loaded by all RBs at any time. Therefore, four sub-bands contain 17 RBs and two sub-bands contain 16 RBs. The coverage area of the first sector ($0 < r \leq R_m, -\pi/6 \leq \theta \leq \pi/6$) is analyzed, because of symmetry the same results are obtained for other sectors.

At first, we calculate the throughput of macrocell network. We carry out simulations for 10^5 Monte Carlo trials where in each trial shadowing and multipath effects change according to the mentioned models. MUE is uniformly located in the coverage area of the first sector.

For comparison, we consider three-sector macrocell scheme which comprises of three 120° antennas to coverage the hexagonal area as shown in Fig. 5. In this case, the available spectrum is divided into three equal sub-bands where two sub-bands contain 33 RBs and one sub-band contains 34 RBs. The cumulative distribution function (CDF) of throughput as a performance metric is demonstrated in Fig. 6 for six- and three-sector macrocells. It is observed that the CDF of six-sector macrocell throughput has smaller values than that of the three-sector macrocell. Since six-sector macrocell has lower interference values in comparison with three-sector macrocell, the SIR of MUE increases which results in higher throughput.

As mentioned previously, it is assumed that femtocells do not have effect on each others. According to the proposed channel assignment allocation to the femtocells, there are 83 ($=17 \times 3 + 2 \times 16$) RBs available to each femtocell in the coverage area of the first sector.

In order to compute the throughput of the femtocell network, 20 FAPs are placed randomly in different locations of the first sector for 200 times. For each FAP location, FUE is located at the border of femtocell to consider the worst case scenario in which FUE receives the

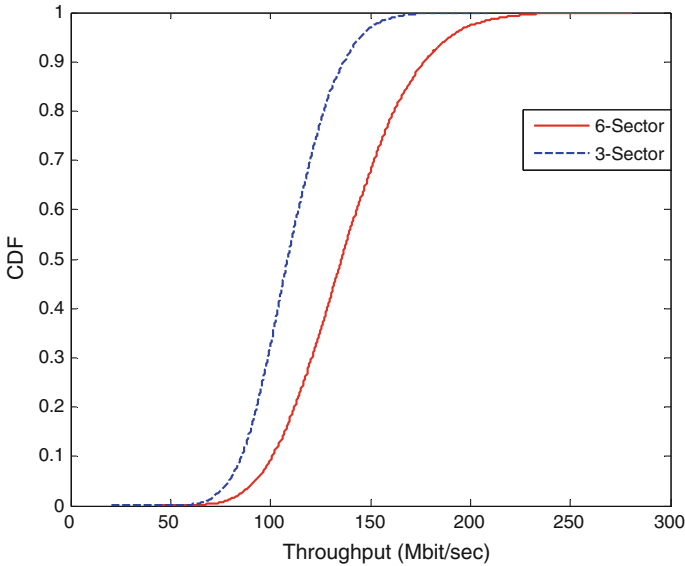


Fig. 6 Comparison between the CDFs of throughputs of fully loaded six-sector and three-sector macrocells

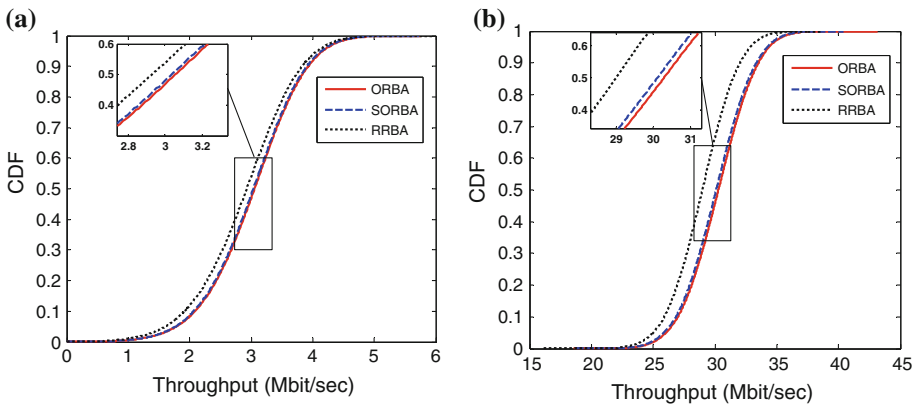


Fig. 7 CDF of femtocell throughput for the worst case scenario when FUE uses 1 and 10 RBs. a 1RB, b 10RBs

lowest power from FAP. For each FAP location, the throughput of FUE is calculated 10^5 times to consider the random effects of shadowing and multipath. In order to allocate RB to FAP, three different algorithms are used: RRBA, SORBA, and ORBA.

In Figs. 7 and 8, the efficiency of these algorithms for the worst case of throughput when FUE uses 1, 10, and 20 RBs, are shown. When the number of RBs used by FUE is low, there is no considerable difference between the throughputs of ORBA and SORBA algorithms. If the number of RBs increases, the difference between their throughputs increases. Also, ORBA and SORBA have higher throughputs than RRBA for all number of RBs. The results indicate that when more information about the location of the FAP is available; the throughput of the femtocell can be improved using better interference management.

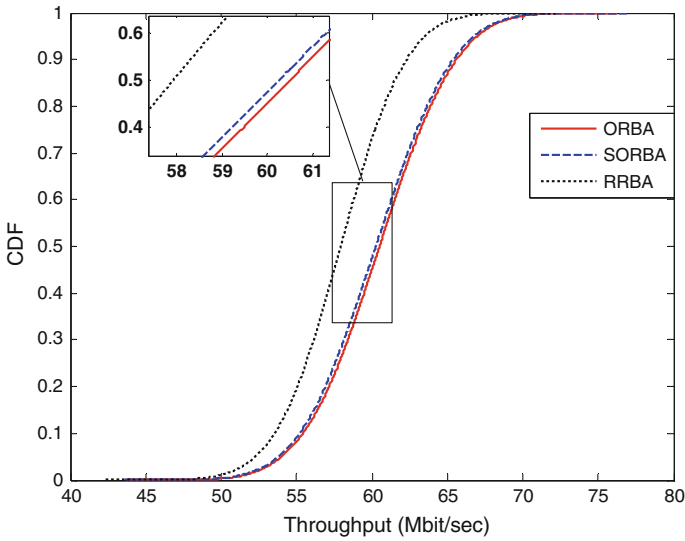


Fig. 8 CDF of femtocell throughput for the worst case scenario when FUE uses 20 RBs

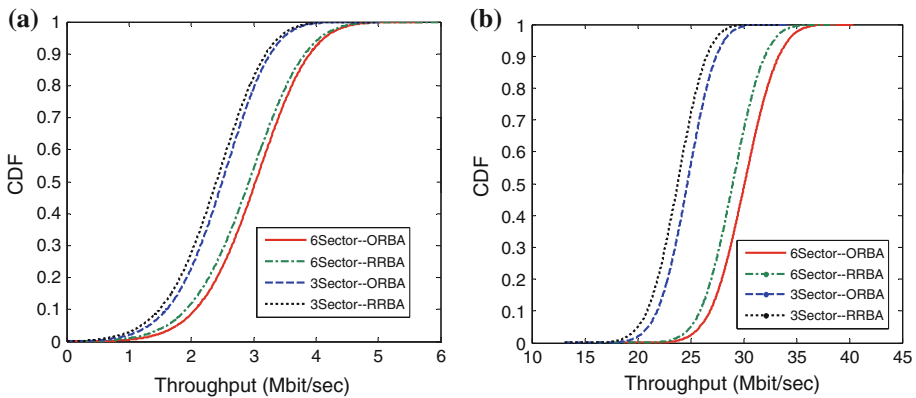


Fig. 9 Comparison between the throughputs of femtocell network in three-sector and six-sector macrocell layouts. **a** 1 RB, **b** 10 RBs

The throughput of femtocell in the six-sector macrocell is compared with that of three-sector macrocell for ORBA and RRBA algorithms. In three-sector macrocell, the number of available RBs in each sector is 66 ($=33 \times 2$), which is smaller than the 84 RBs in six-sector macrocell case. In Fig. 9, the CDF of throughput of the worst case scenario is presented for three-sector and six-sector macrocell layouts. We observe that RRBA allocation in six-sector layout can provide better throughput for femtocell than the ORBA allocation in three-sector layout. This is because of more cross-tier interference reduction in six-sector macrocell compared with the three-sector macrocell. Since FAP transmits low power, cross-tier interference reduction can cause considerable increment in the downlink SIR of femtocell users.

The outage probability of the femtocell is also obtained based on the distance of FUE from MBS of M_0 . In a specific distance from the MBS, 20 different angles are considered and the obtained results are averaged. FUE is considered at the edge of femtocell and for each

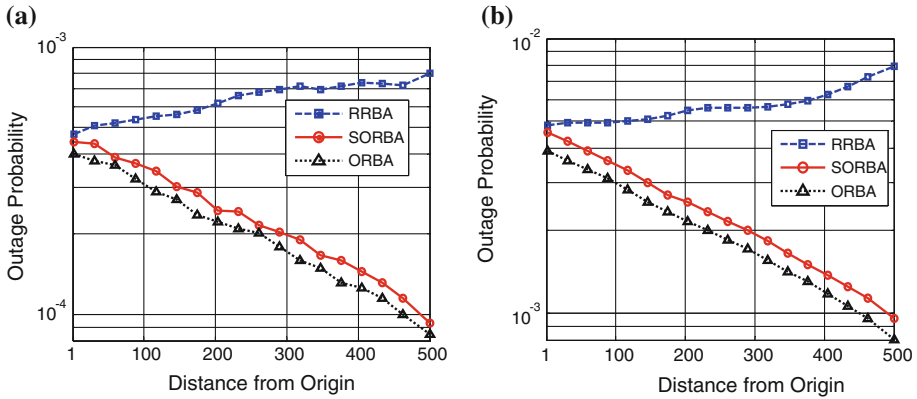


Fig. 10 Outage probability of femtocell for different number of RBs. a 1 RB, b 10 RBs

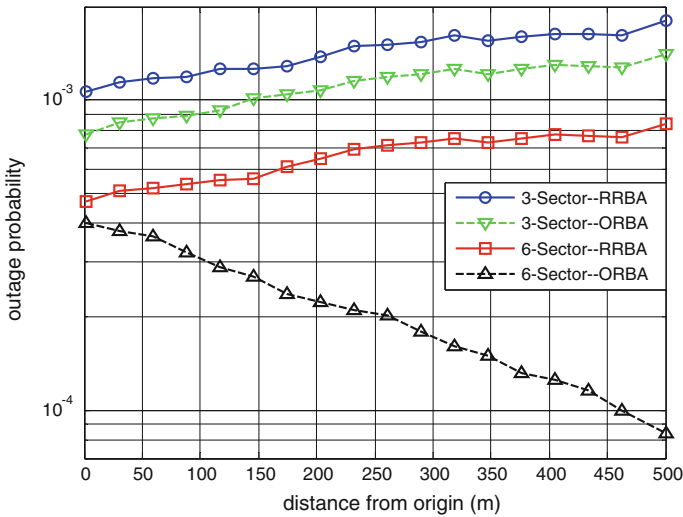


Fig. 11 OPs of femtocell network in three-sector and six-sector macrocell layouts for one RB

FUE location, the OP is computed 10^5 times to consider the effect of random shadowing and fast fading. The results are demonstrated in Fig. 10. We observe that ORBA and SORBA have lower outage probabilities than the RRBA due to the more interference reduction. Also, in Fig. 11 the outage probability of femtocell network is depicted for both three-sector and six-sector macrocell layouts. It is observed that six-sector layout has lower outage probability and can provide better service to FUE.

7 Conclusion

In this paper, co-tier and cross-tier interference issues in six-sector macrocells overlaid with femtocells were analyzed. The results showed that if the number of sectors in MBS increases, co-tier interference in macrocell network reduces which increases the throughput of macrocell network. It was demonstrated that FUE receives different cross-tier interferences in different sub-bands allocated to macrocell in different sectors and the order of interferences

changes in different user locations. Therefore, if the location of FAP is known, interference management algorithms can improve throughput and outage probability of femtocell network. Consequently, it was proposed when FAP connects to backhaul network, RNC sends the priority of sub-bands. The priority is determined in a manner that minimizes the cross-tier interference from macrocell to femtocell. Then, according to proposed low-interference RB allocation algorithm, FAP starts allocating RBs with low interference sub-bands to FUE. Experimental results showed that more information about FAP location can provide more information about the order of interferences which results in more cross-tier interference reduction in the FUE. More information about FAP location improves the throughput and outage probability of femtocell network.

In this paper, in order to allocate RB to FAP, only the received interference is considered and all RBs of each sub-band have the same priority. In the future works, we will analyze the link between the FAP and FUE to assign the best RB from the low-interference sub-band. Further, the case of high dense femtocell network should be analyzed, in which the femto to femto cannot be ignored.

Acknowledgments This work was supported by Iran Research Institute for ICT-ITRC under Contract No. 50014813.

References

- Chandrasekhar, V., Andrews, J., & Gatherer, A. (2008). Femtocell networks: A survey. *IEEE Communications on Magazine*, 46(9), 59–67.
- Chandrasekhar, V., & Andrews, J. (2009). Spectrum allocation in tiered cellular networks. *IEEE Transactions on Communications*, 57(10), 3059–3068.
- Chowdhury, M. Z., Jang, Y. M., & Haas, Z. J. (2011). Cost-effective frequency planning for capacity enhancement of femtocellular networks. *Wireless Personal Communications*, 60(1), 83–104.
- Jo, H.-S., Mun, C., Moon, J., & Yook, J.-G. (2009). Interference mitigation using uplink power control for two-tier femtocell networks. *IEEE Transactions on Wireless Communications*, 8(10), 4906–4910.
- Tariq, F., Dooley, L. S., Poulton, A. S., & Ji, Y. (2011). Dynamic fractional frequency reuse based hybrid resource management for femtocell networks. In *International wireless communications and mobile computing conference (IWCMC)*, pp. 272–277.
- Wu, J. Y., Chu, X., & Lopez-Perez, D. (2012). Downlink outage probability of co-channel femtocells in hierarchical 3-sector macrocells. *IEEE Communications Letters*, 16(5), 698–701.
- Oh, C.-Y., Chung, M. Y., Choo, H., & Lee, T.-J. (2013). Resource allocation with partitioning criterion for macro–femto overlay cellular networks with fractional frequency reuse. *Wireless Personal Communications*, 68(2), 417–432.
- Yavuz, M., Meshkati, F., Nanda, S., Pokhariyal, A., Johnson, N., Raghothaman, B., et al. (2009). Interference management and performance analysis of UMTS/HSPA+ femtocells. *IEEE Communications on Magazine*, 47(9), 102–109.
- Zhao, G., Yang, C., Li, G. Y., & Sun, G. (2011). Fractional frequency donation for cognitive interference management among femtocells. In *IEEE global telecommunications conference (GLOBECOM)*, pp. 1–6.
- Lee, H.-C., Oh, D.-C., & Lee, Y.-H. (2010). Mitigation of inter-femtocell interference with adaptive fractional frequency reuse. In *IEEE international conference on communications (ICC)*, pp. 1–5.
- Lee, J. Y., Bae, S. J., Kwon, Y. M., & Chung, M. Y. (2011). Interference analysis for femtocell deployment in OFDMA systems based on fractional frequency reuse. *IEEE Communications on Letters*, 15(4), 425–427.
- López-Pérez, D., de la Roche, G., Valcarce, A., Juttner, A., & Zhang, J. (2008). Interference avoidance and dynamic frequency planning for WiMAX femtocells networks. In *IEEE Singapore international conference on communication systems*, pp. 1579–1584.
- Yun, J.-H., & Shin, K. G. (2011). Adaptive interference management of OFDMA femtocells for co-channel deployment. *IEEE Journal on Selected Areas in Communications*, 29(6), 1225–1241.
- 3GPP. (2008). *E-UTRA and E-UTRAN overall description; stage 2 (release 8)*. Technical specification. TS 36.300 V8.7.0.
- Astély, D., Dahlman, E., Furuskar, A., Jading, Y., Lindstrom, M., & Parkvall, S. (2009). LTE: The evolution of mobile broadband. *IEEE Communications on Magazine*, 47(4), 44–51.

16. Recommendation, I. (1997). *1225, Guidelines for evaluation of radio transmission technologies for IMT-2000*. International Telecommunication Union.
17. Lee, T., Yoon, J., Lee, S., & Shin, J. Interference management in OFDMA femtocell systems using fractional frequency reuse. (2010). In *IEEE international conference on communications, circuits and systems (ICCCAS)*, pp. 176–180.
18. Huang, H., Alrabadi, O., Daly, J., Samardzija, D., Tran, C., Valenzuela, R., et al. (2010). Increasing throughput in cellular networks with higher-order sectorization. In *Asilomar conference on signals, systems and computers (ASILOMAR)*, pp. 630–635.
19. Claussen, H. (2008). Co-channel operation of macro- and femto-cells in a hierarchical cell structure. *International Journal of Wireless Information Networks*, 15(3), 137–147.

Author Biographies



Hashem Kalbkhani received the B.S. and M.S. from Urmia University, Iran, both in Electrical Engineering. He is currently working toward Ph.D. program at the Department of Electrical Engineering, Urmia University, Urmia, Iran. His research interest are wireless communication, cellular networks especially in interference, resource, and handover management in small cell environments, signal processing, and image processing.

Sahar Jafarpour-Alamdari received the B.S. degree from University of Tabriz, Iran, and M.S. degree from Urmia University, Iran both in Electrical Engineering. Her research interests include wireless communication, handoff and resource management in cellular networks.



Vahid Solouk received his B.Sc. from Urmia University, Iran and his M.Sc. from Najafabad University, Iran, and the degree of Ph.D. from Universiti Putra, Malaysia, all in communication and electrical engineering. He is currently with the Department of IT and Computer Engineering, Urmia University of Technology, Urmia, Iran. He was with Telecommunication Company of Iran and UNHCR specifically in Mobile Communication and Data Network Departments. His major areas of interest are wireless communication and networking particularly in integration and interworking, mobility and resource management, and simulation and prototyping in cellular and WLAN networks.

Mahrokh G. Shayesteh received the B.Sc. from University of Tehran, Iran, the M.Sc. from Khajeh Nassir University of Technology, Iran, and the degree of Ph.D. from Amir Kabir (Tehran Polytechnic) University of Technology, Iran, all in electrical engineering. She is currently with the Department of Electrical Engineering, Urmia University, Urmia, Iran. She is also working with the Wireless Research Laboratory, Advanced Communication Research Institute (ACRI), Department of Electrical Engineering, Sharif University of Technology, Tehran. Her research interests include wireless communication systems, cellular networks, spread spectrum, UWB, and image processing.